Thermal oxidation of carbothermal β′-sialon powder: reaction sequence and kinetics

Kenneth J. D. MacKenzie,*[a] Shiro Shimada[b] and Takenori Aoki[b]

[a]*New Zealand Institute for Industrial Research and Development, P.O. Box 31–310 Lower Hutt, New Zealand*
[b]*Faculty of Engineering, Hokkaido University, Sapporo 060, Japan*

The oxidation of carbothermally synthesised β′-sialon powder ($z=2.45$) was found by X-ray powder diffraction and solid-state ^{29}Si and ^{27}Al MAS NMR spectroscopies to result in the initial formation of amorphous SiO_2 and a non-crystalline mullite-like aluminosilicate which becomes crystalline at higher temperatures. The evolution of crystalline mullite is accompanied by a decrease in both the sialon z value and in the proportion of tetrahedral Al. The ratio of ^{29}Si in the SiO_2 to ^{29}Si in the mullite oxidation products is about 4, consistent with the formation of Al_2O_3 as an additional oxidation product. The oxidation kinetics at 1100–1300 °C are described by a parabolic rate law with an activation enthalpy of 161 kJ mol^{-1}, suggesting the rate-determining step to be the permeation of oxygen through the oxidised layer coating the sialon grains.

Many applications for advanced ceramics call for their use at elevated temperatures in air. The thermal oxidation of non-oxide ceramics such as silicon nitride and sialons is therefore a limiting factor in such applications, although in practice the progress of oxidative degradation can be slowed significantly by the limited access of air in highly dense bodies, and, in silicon nitride, by the formation of a structurally dense subsurface Si_2N_2O layer interposed between the bulk Si_3N_4 and the SiO_2 oxidation product.[1] Of the many published kinetic studies of Si_3N_4 oxidation,[2–7] most were performed on dense sintered bodies which contained sintering additives such as MgO[2–4] or rare-earth-metal oxides[5] which influence the rate of the typically parabolic oxidation kinetics by becoming incorporated in the subsurface interface layer.[5] The one published study of the oxidation kinetics of undoped Si_3N_4 powder[6] should represent a limiting case of the fastest reaction parameters uncomplicated by side reactions, and provide a benchmark against which more slowly oxidising systems may be compared. More recently, the oxidation of Si_3N_4 powder containing 4 mass% Y_2O_3[7] has indicated the role played by the lanthanide in forming an interfacial phase below the surface SiO_2 layer.

By comparison with silicon nitride, the oxidation of sialon has been much less thoroughly studied. Singhal and Lange[8] reported that the oxidation of hot-pressed sialon compacts followed a parabolic rate law, with increased oxidation resistance as the Al content increased. Mullite ($Al_6Si_2O_{13}$) was the only identifiable crystalline oxidation product. Work by Chartier *et al.*[9] on β′-sialon ($z=0.4$) sintered with 14 mass% Y_2O_3 suggests that in such samples the oxidation kinetics are controlled by yttrium migration in the intergranular glassy phase.

The aim of the present work is to establish the oxidation kinetics of undoped β′-sialon powder as a baseline against which more oxidation-resistant sialon systems may subsequently be compared, and to investigate the formation of both the crystalline and non-crystalline product phases using X-ray powder diffraction (XRD) and ^{29}Si and ^{27}Al solid-state MAS NMR respectively.

Experimental

The β′-sialon was synthesised from high purity New Zealand halloysite clay by carbothermal reduction, as described elsewhere.[10] XRD showed it to be predominantly monophasic with $z=2.45$ and a particle size distribution, determined by laser interferometry, of 100% < 6 μm, 50% < 2 μm, 10% < 1 μm. Chemical analysis by X-ray fluorescence spectrometry indicated the following typical impurity levels (in elemental mass%), carried over from the clay starting material: 0.13% Fe, 0.03% Ti, 0.06% Ca, < 0.01% K, < 0.005% Mg, < 0.001% Cr. The only impurity phase detectable by XRD was a trace of X-phase sialon, with no evidence of glass. Samples (1.0 g) were oxidised in air at 950–1400 °C for 1 h in platinum crucibles, using an electric muffle furnace. The powders were then examined by XRD (Philips PW 1700 computer-controlled diffractometer with graphite monochromator and Co-Kα radiation). The ^{29}Si and ^{27}Al MAS NMR spectra were obtained at 11.7 T using a Varian Unity 500 spectrometer and a 5 mm Doty MAS probe spun at 10–12 kHz under the following conditions: ^{29}Si: 6 μs $\pi/2$ pulse, recycle delay 300 s, shifts referenced to tetramethylsilane; ^{27}Al: 1 μs $\pi/10$ pulse for solution, recycle delay 5 s, shifts referenced to 1 mol dm^{-3} aqueous $Al(NO_3)_3$ solution.

The oxidation kinetics were measured by isothermal thermogravimetry of the sialon powder at 1105–1305 °C in a Rigaku thermoanalyser with an infrared image furnace. Samples (50 mg) were brought to the reaction temperature at 20 °C min^{-1} under a flowing Ar atmosphere, then, after equilibration, the atmosphere was changed to flowing air (200 ml min^{-1}), this point being taken as $t=0$ in the kinetic experiment. The oxidation mass change was then monitored continuously for the duration of the experiment (2 h).

Results and Discussion

Oxidation reaction

Fig. 1 shows the relative intensities of the major XRD diffraction lines for the various crystalline phases identified in samples oxidised between 950 and 1400 °C. The diffraction peaks used in this diagram were: β′-sialon: JCPDF no. 36–1333, 3.32 Å (020); mullite: JCPDF no. 15–776, 3.38 Å (210); cristobalite: JCPDF no. 11-695, 4.04 Å (101); X-phase sialon: JCPDF no. 36-832, 3.62 Å (320).

Between room temperature and 950 °C, the intensity of the β′-sialon diffraction pattern shows only a very slight decrease, but above 950 °C, the intensity decreases regularly, with a plateau at *ca.* 1150–1200 °C (Fig. 1). The small amount of X-phase present appears to be more resistant to low-temperature oxidation, its intensity remaining virtually unchanged until its abrupt disappearance < 1150 °C (Fig. 1).

Fig. 2 shows the changes during oxidation of the mean z value of the sialon phase, deduced by the method of Ekström *et al.*[11] from careful measurements of the a and c cell parameters using elemental Si as the external calibration standard.

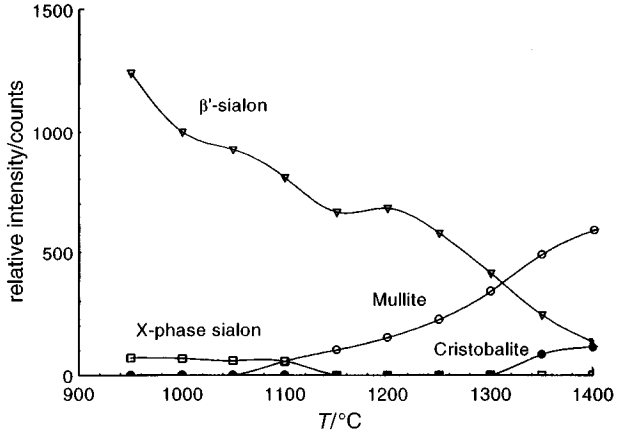

Fig. 1 Semi-quantitative representation of the phases in carbothermal β′-sialon powder as a function of the oxidation temperature, 1 h holding time at each temperature

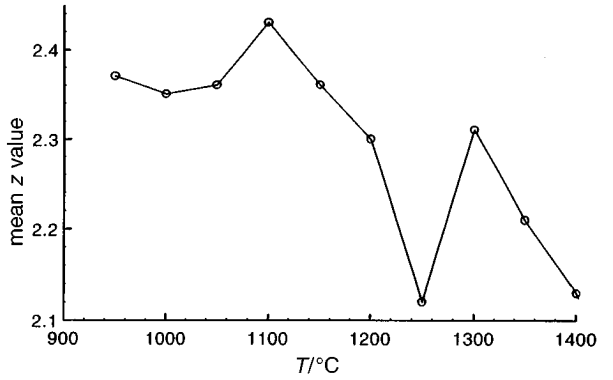

Fig. 2 Mean z value of carbothermal β′-sialon powder as a function of oxidation temperature, 1 h holding time at each temperature

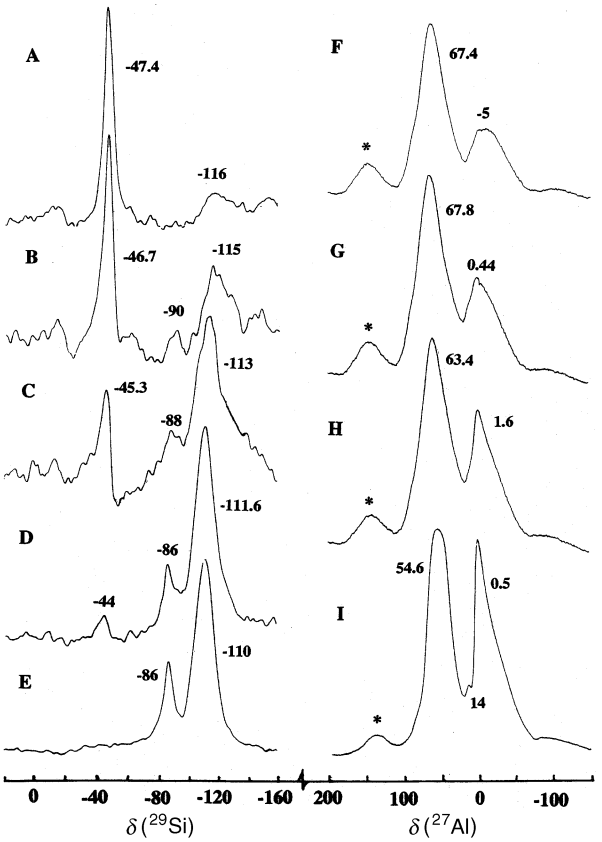

Fig. 3 Typical 11.7 T MAS NMR spectra of carbothermal β′-sialon powder oxidised for 1 h at the indicated temperatures. A–E, ^{29}Si spectra (A, unheated; B, 950 °C; C, 1000–1100 °C; D, 1100–1200 °C; E, 1300–1400 °C); F–I, ^{27}Al spectra (F, unheated; G, 950–1000 °C; H, 1050–1200 °C; I, 1250–1400 °C). Asterisks indicate spinning side bands.

The experimental error in these measurements will be greatest at the higher oxidation temperatures, owing to the weaker diffraction patterns as the sialon phase disappears; nevertheless, the results indicate a decrease in the amount of aluminium in the sialon as oxidation proceeds, with an apparent discontinuity at *ca.* 1250 °C.

The early stages of oxidation are not accompanied by the appearance of any crystalline oxidation product; mullite makes its appearance at 1100 °C (Fig. 1), and grows steadily in intensity and crystallinity above that temperature. Careful measurements of the cell parameters of the evolving mullite, made using elemental Si as the external calibration standard, were used to deduce the composition of the mullite, from the relationship of Cameron.[12] The least reliable results for this phase were those of the lower-temperature samples, in which the mullite was only poorly crystalline. Using the measured mullite cell volumes, the mullite composition was found in most of the samples to be 60.2–62.0 mol% Al_2O_3, *i.e.* corresponding to 3:2 mullite. The alumina contents deduced from the mullite a parameters alone were slightly poorer in alumina. No trend was found between the alumina content of the mullite and the oxidation temperature.

Above 1300 °C, a small amount of crystalline cristobalite (SiO_2) becomes evident (Fig. 1). A selection of typical ^{29}Si and ^{27}Al MAS NMR spectra of the oxidised sialons are shown in Fig. 3.

During the course of oxidation, the ^{29}Si spectra show a progressive intensity decrease of the diagnostic peak for β′-sialon, which occurs at δ −47.6 to −48.4.[13] The progressive downfield shift of this peak during oxidation is apparently real, but the reason is not presently understood. The broad feature at δ −116 in the unheated sialon (Fig. 3A) is due to a small amount of uncombined amorphous silica; this resonance increases markedly from the first stages of oxidation, becoming narrower and shifting at higher temperatures towards the reported value for cristobalite (δ −108.5).[14] Another small resonance at δ −88 to −90, which can be discerned even at the lowest oxidation temperature used here, evolves at higher temperatures into a sharp peak corresponding to the major resonance of mullite (δ −86.4[15]). Thus, from the onset of oxidation, both amorphous silica and a trace of an aluminosilicate similar to mullite are detected by ^{29}Si NMR spectroscopy but not by XRD. By 1100 °C, the mullite structure has become sufficiently organised for XRD detection, but the silica oxidation product remains X-ray amorphous until 1300 °C, when some is converted to cristobalite. These changes were charted by integration of the ^{29}Si spectra over the diagnostic spectral regions of the three Si-containing phases, to give a representation of the changes in partitioning of Si within the system during oxidation (Fig. 4).

Fig. 4 indicates that the ratio of Si in SiO_2 to Si in mullite is about 4 at 1400 °C. On this basis, the oxidation reaction approximates to:

$$6Si_7Al_5O_5N_{11} \xrightarrow{O_2} 4Al_6Si_2O_{13} + 34SiO_2 + 3Al_2O_3 + 33N_2 \quad (1)$$

giving a predicted ratio of Si in SiO_2 to Si in mullite of 4.25, and indicating the formation of some Al_2O_3. Although XRD evidence for the latter is lacking, the ^{27}Al spectra of samples heated to higher temperatures confirm the presence of a small amount of alumina (see below). No NMR evidence was found for the significant formation of oxynitride intermediates in the oxidation process.

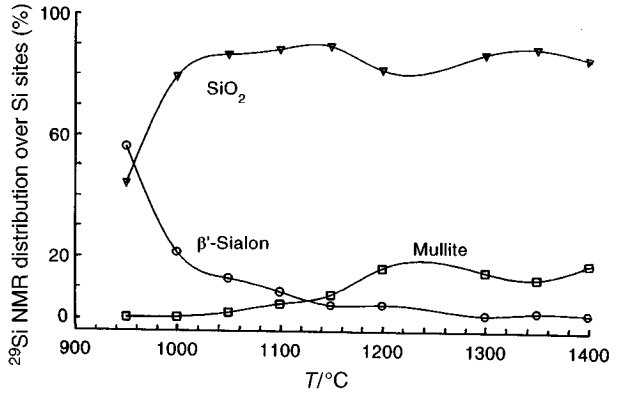

Fig. 4 Partitioning of ^{29}Si over the various phases in oxidised carbothermal β′-sialon powder as a function of oxidation temperature

The ^{27}Al spectra (Fig. 3F–I) show a change in the ratio of tetrahedral Al sites (at δ *ca.* 55 to 68) to octahedral (δ −5 to 1.6) as oxidation proceeds. The change in the position and shape of the tetrahedral peak corresponds to the conversion of Al in β′-sialon (δ 66–69[13]) to mullite, in which two tetrahedral peaks can sometimes be resolved, at δ 42.2–48.3 and 56.6–66.1.[15] The position and squarish shape of the tetrahedral Al peaks in the present samples oxidised at 1250–1400 °C (Fig. 3I) reflects these two unresolved tetrahedral sites. The proportion of tetrahedral sites, determined by curve-fitting the ^{27}Al spectra, decreases progressively as oxidation progresses, achieving a high-temperature value (52%) consistent with that deduced from the published 11.7 T spectrum of sintered synthetic mullite.[15]

At the higher oxidation temperatures, an additional small resonance appears at δ *ca.* 14 (Fig. 3I); this arises from a small amount of α-Al_2O_3, present in too small a concentration to be detected by XRD.

In summary, the combined XRD and NMR evidence indicates that undoped β′-sialon powder oxidises at >900 °C with the formation of X-ray amorphous SiO_2, the associated Al residing in aluminosilicate regions which subsequently form crystalline mullite >1050 °C. During oxidation, the Al content of the sialon, as reflected in its *z* value, decreases slightly, although the Al content of the mullite product remains constant at about the 3:2 mullite composition. The concentration of excess Al is insufficient to be detected by XRD, but appears at higher temperatures in the ^{27}Al NMR spectrum as α-Al_2O_3. Crystalline SiO_2 (cristobalite) is also detected at higher temperatures. No evidence was found for the formation of significant oxynitride intermediates in the oxidation process.

Oxidation kinetics

The isothermal mass-gain curves for five oxidation temperatures are shown in Fig. 5. These were analysed in terms of the parabolic rate law which has been found most frequently to describe the oxidation behaviour of sialons and Si_3N_4:

$$\Delta m^2 = kt + c \quad (2)$$

where Δm is the oxidation mass change per unit area, k is the reaction rate constant and c is a numerical constant. Scanning electron micrographs of the unoxidised and variously oxidised samples indicated clearly that the particle size and morphology are unchanged over the temperature range of the kinetic experiments, consistent with the well known difficulty of sintering undoped β′-sialon. For the purpose of this kinetic analysis, the particle area was therefore treated as a constant.

Eqn. (2) was found to fit the present data reasonably well, although, as was found for the oxidation of Si_3N_4 powder,[6] the results suggest an initial induction period which may be due to the presence of an oxidised layer on the original particles, or to genuine initial linear oxidation behaviour, or both. The parabolic rate law was also found to describe the initial portions of the kinetic curves reasonably well, and gave a similar activation enthalpy; the full data set was therefore used to determine the parabolic rate constants, shown in Fig. 6.

The slope of the resulting Arrhenius plot (Fig. 7) gave a value for the activation enthalpy (temperature dependence of the oxidation rate) of 161 kJ mol^{-1}. This enthalpy is low by

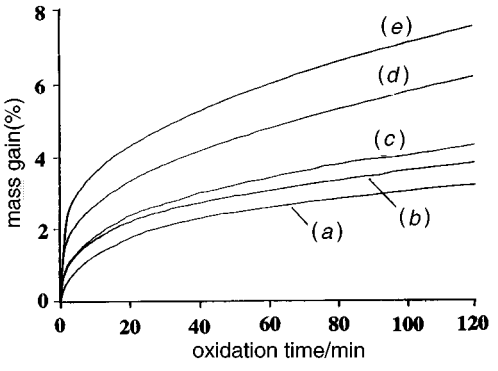

Fig. 5 Isothermal oxidation curves for carbothermal β′-sialon powder in air: (*a*) 1105 °C; (*b*) 1150 °C; (*c*) 1175 °C; (*d*) 1260 °C; (*e*) 1305 °C

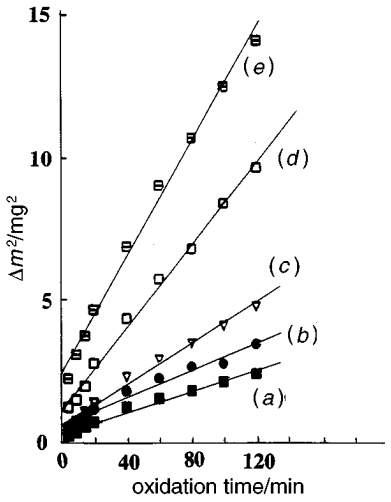

Fig. 6 Kinetic data for oxidation of carbothermal β′-sialon powder plotted according to the parabolic rate law: (*a*) 1105 °C; (*b*) 1150 °C; (*c*) 1175 °C; (*d*) 1260 °C; (*e*) 1305 °C

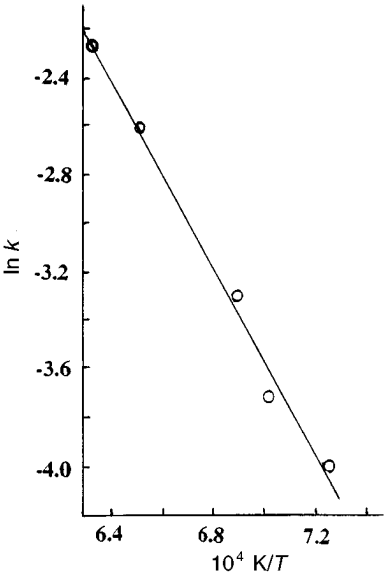

Fig. 7 Arrhenius plot for oxidation of carbothermal β′-sialon powder

comparison with the only other literature value for β′-sialon (440 kJ mol^{-1}).[9] The samples used in that study were, however, very different, being sintered bodies of $z=0.4$, containing Y_2O_3 as a sintering additive, all of which factors are expected to affect the oxidation kinetics; sintered bodies oxidise more slowly than powders, whereas the oxidation rate decreases with decreasing z value.[8] Additives such as Y_2O_3 are reported to give rise to linear rather than parabolic kinetics in Si_3N_4 powders,[7] and might exert a similar influence on sialon powders. For these reasons, a more meaningful comparison might be made with undoped Si_3N_4 powder, for which activation enthalpies ranging from 147[16] to 285 kJ mol^{-1} [6] have been reported. As expected, these activation enthalpies are generally lower than the range reported for sintered Si_3N_4 compacts (293[3] to 440 kJ mol^{-1} [4]), but since these samples normally contain oxide sintering additives which are known to enter into the oxidation process, the relative effects of densification and sintering additive on the oxidation kinetics are difficult to distinguish. An even greater spread of activation enthalpies has been reported for the oxidation of Si_3N_4 CVD films (88 to 628 kJ mol^{-1} [17]).

The rather low activation enthalpy found for the present samples is of similar magnitude to that reported for the diffusion of oxygen in fused SiO_2 (122 kJ mol^{-1} [18]), suggesting that in our β′-sialon powder containing no additives, the rate-determining process might be the diffusion of oxygen through the SiO_2 surface layers. Alternatively, oxygen diffusion through mullite may be a rate-determining process in sialon oxidation, since mullite is another principal product. Data for oxygen self-diffusion in mullite are not available, but oxygen ion conductivity measurements in mullite[19,20] indicate an activation enthalpy which is dependent on the thermal history, and ranges from 63 to 112 kJ mol^{-1} for undoped 3:2 mullite. These enthalpies can be equated to the activation enthalpy for random diffusion of oxygen in mullite, and their similarity to the present oxidation enthalpy, while tending to confirm oxygen diffusion as rate determining, militate against an unambiguous identification of the phase presenting the diffusion barrier.

From absolute rate theory,[21] the Gibbs activation energy ΔG^* and activation entropy ΔS^* are given by:

$$\Delta G^* = RT[\ln(RT/Nh) - \ln k] \quad (3)$$

$$\Delta S^* = (E_a - \Delta G^*)/T \quad (4)$$

where R is the gas constant, N is Avogadro's number and h is Planck's constant.

The values of ΔG^* thus calculated fall in the range 504–587 kJ mol^{-1}, and the ΔS^* values fall in the range −249 to −271 J K^{-1} mol^{-1}. The negative value of the activation entropy is consistent with the transition state being substantially more ordered than the reactants, as would be expected for sorption of oxygen on to the surface of the sialon grains.

Conclusions

β′-Sialon powder ($z=2.45$) produced by carbothermal synthesis oxidised in air above 900 °C with the initial formation of amorphous SiO_2 and an aluminosilicate with NMR characteristics similar to mullite, but only acquiring sufficient ordering to be detected by XRD above 1100 °C. At higher temperatures (>1300 °C) some of the amorphous silica is converted to crystalline cristobalite.

As the reaction proceeds, the sialon z value decreases, with a discontinuity at 1250 °C. The proportion of tetrahedral Al (deduced by ^{27}Al MAS NMR spectroscopy) decreases progressively with temperature, to a value consistent with crystalline 3:2 mullite.

At 1400 °C the distribution of ^{29}Si in the two principal oxidation products (SiO_2 and mullite) suggests Al_2O_3 should be a further reaction product; this phase was detected by ^{27}Al MAS NMR spectroscopy but not by XRD.

The oxidation kinetics of carbothermally synthesised β′-sialon powder at 1100–1300 °C can be described by a parabolic rate law with an activation enthalpy E_a of 161 kJ mol^{-1} and a negative activation entropy. The E_a value is similar to that for oxygen diffusion in both SiO_2 and mullite, suggesting that the rate-determining step is the permeation of oxygen through the oxidised product layer coating the sialon grains.

References

1 H. Du, R. E. Tressler and K. E. Spear, *J. Electrochem. Soc.*, 1989, **136**, 3210.
2 S. C. Singhal, *J. Mater. Sci.*, 1976, **11**, 500.
3 W. C. Tripp and H. C. Graham, *J. Am. Ceram. Soc.*, 1976, **59**, 399.
4 D. Cubicciotti and K. H. Lau, *J. Am. Ceram. Soc.*, 1978, **61**, 512.
5 D. M. Mieskowski and W. A. Sanders, *J. Am. Ceram. Soc.*, 1985, **68**, C160.
6 R. M. Horton, *J. Am. Ceram. Soc.*, 1969, **52**, 121.
7 P. S. Wang, S. M. Hsu, S. G. Malghan and T. N. Wittberg, *J. Mater. Sci.*, 1991, **26**, 3249.
8 S. C. Singhal and F. F. Lange, *J. Am. Ceram. Soc.*, 1977, **60**, 190.
9 T. Chartier, J. L. Besson and P. Goursat, *Int. J. High Tech. Ceram.*, 1986, **2**, 33.
10 K. J. D. MacKenzie, R. H. Meinhold, G. V. White, C. M. Sheppard and B. L. Sherriff, *J. Mater. Sci.*, 1994, **29**, 2611.
11 T. Ekström, P. O. Kall, M. Nygren and P. O. Olsson, *J. Mater. Sci.*, 1989, **24**, 1853.
12 W. E. Cameron, *Am. Ceram. Soc. Bull.*, 1977, **56**, 1003.
13 J. Sjöberg, R. K. Harris and D. C. Apperley, *J. Mater. Chem.*, 1992, **2**, 433.
14 J. V. Smith and C. S. Blackwell, *Nature* (*London*), 1983, **303**, 223.
15 L. H. Merwin, A. Sebald, H. Rager and H. Schneider, *Phys. Chem. Miner.*, 1991, **18**, 47.
16 P. Goursat, P. Lortholary, D. Tetard and M. Billy, *Proc. Int. Symp. React. Solids, Bristol, 1972*, ed. J. S. Anderson, Chapman and Hall, London, 1972, pp. 315–326.
17 J. D. Choi, D. B. Fischbach and W. D. Scott, *J. Am. Ceram. Soc.*, 1989, **72**, 1118.
18 E. L. Williams, *J. Am. Ceram. Soc.*, 1965, **46**, 190.
19 G. Meng and R. A. Huggins, *Solid State Ionics*, 1984, **11**, 271.
20 G. Meng, W. Cao and D. Peng, *Solid State Ionics*, 1986, **18&19**, 732.
21 H. Eyring, *J. Chem. Phys.*, 1935, **3**, 107.

Paper 6/04354B; *Received* 24*th June*, 1996